APPLIED AND ENVIRONMENTAL MICROBIOLOGY, May 2002, p. 2468–2478 Vol. 68, No. 5
0099-2240/02/$04.00+0 DOI: 10.1128/AEM.68.5.2468–2478.2002

Energy-Based Dynamic Model for Variable Temperature Batch Fermentation by *Lactococcus lactis*†

Daniel P. Dougherty,[1,2] Frederick Breidt, Jr.,[1,2]* Roger F. McFeeters,[1,2] and Sharon R. Lubkin[3]

U.S. Department of Agriculture, Agricultural Research Service,[1] and North Carolina Agricultural Research Service,[2] Department of Food Science, North Carolina State University, Raleigh, North Carolina 27695-7624, and Departments of Statistics and Mathematics, North Carolina State University, Raleigh, North Carolina 27695-8203[3]

Received 9 July 2001/Accepted 14 February 2002

We developed a mechanistic mathematical model for predicting the progression of batch fermentation of cucumber juice by *Lactococcus lactis* under variable environmental conditions. In order to overcome the deficiencies of presently available models, we use a dynamic energy budget approach to model the dependence of growth on present as well as past environmental conditions. When parameter estimates from independent experimental data are used, our model is able to predict the outcomes of three different temperature shift scenarios. Sensitivity analyses elucidate how temperature affects the metabolism and growth of cells through all four stages of fermentation and reveal that there is a qualitative reversal in the factors limiting growth between low and high temperatures. Our model has an applied use as a predictive tool in batch culture growth. It has the added advantage of being able to suggest plausible and testable mechanistic assumptions about the interplay between cellular energetics and the modes of inhibition by temperature and end product accumulation.

A number of models have been developed to predict the growth of bacteria in foods (3, 21, 24). Several common types of these growth models, including the logistic, Gompertz, and Richards curves, have been shown to be special cases of a more general model (2, 27, 28). These models may be classified as empirical models; they are sigmoidal functions that approximate bacterial growth over time. It has been argued, however, that the usefulness of empirical models is limited and that a more fundamental understanding of the changes taking place during batch growth of bacteria will require the use of mechanistic models (2, 20, 31). A drawback of most of the above models is the assumption of a constant environment during growth, where growth is limited by a time- or cell density-dependent function. From a mechanistic point of view, this is clearly incorrect, as environmental variables, lack of nutrients, and accumulation of end products are the controlling factors in cell growth and death. Both the Monod equation (19), where growth is limited by substrate concentration, and the Levenspiel modification (15), to include end product inhibition, address this issue. These models for the growth of a single organism include a simplifying assumption, however, of a constant relationship between cell numbers, substrate utilization, and inhibitory end product production.

Mechanistic models may be developed from theoretical or experimentally determined data describing the cause or mechanism behind the dynamic changes observed in an experimental system. Several researchers have used dynamic models to investigate the effects of various temperatures on the specific growth rates or lag times of bacterial cultures (3, 4, 9, 29, 30). In all cases, some parameter values in these models were allowed to vary with temperature. Van Impe et al. (29) used temperature-dependent adjustment functions for modifying the parameters for specific growth rate, asymptotic level of (maximum) growth, and lag time with their dynamic model. These functions, suggested by Zwietering et al. (32) for the explicit form of the modified Gompertz equation, were adapted for use with the derivative dynamic model (29, 30). They include the square root model of Ratkowsky et al. (22) for modifying specific growth rate and asymptotic growth parameters with temperature and a hyperbolic function (32) for modifying lag with temperature. The model was validated by studies that compared the observed and predicted growth with *Brochothrix thermosphacta* or *Lactobacillus plantarum* for temperature shifts and continuously varying temperatures during batch growth of these organisms in pure culture (30). Baranyi and Roberts (3), adapted an elegant mechanistic differential equation model (1, 2) for monitoring the growth of *B. thermosphacta* during a time course of changing temperatures. This model used an "adjustment" function that follows Michaelis-Menten-type kinetics to reflect the accumulation of a critical, yet undefined, intracellular component required for cell division. The adjustment function allowed the model to predict growth lag in response to changing environmental conditions. In the temperature-dependent model (3), the parameters for the specific growth rate and the adjustment function were modified by the square root model of Ratkowsky et al. (22) to reflect temperature changes. Validation studies of the temperature-dependent Baranyi model showed very good agreement between the growth of *B. thermosphacta* in broth culture and the predicted results (3). However, this model relied on cell density (intraspecific competition) to limit cell growth. As a direct result, its predictive ability may be limited when applied to environments in which interspecific competition plays an important role (5).

Breidt and Fleming (6) have developed a model that accu-

* Corresponding author. Mailing address: Department of Food Science, North Carolina State University, 322 Schaub Hall, Box 7624, Raleigh, NC 27695-7624. Phone: (919) 515-2979. Fax: (919) 856-4361. E-mail: breidt@ncsu.edu.

† Paper no. FSR01-22 of the Journal Series of the Department of Food Science, North Carolina State University, Raleigh, NC 27695-7624.

TABLE 1. State variables of the model[a]

Symbol	Meaning (unit)	Observed range
t	Time (h)	0–256
T	Temp (°C)	10–30
N	Cell density (CFU ml^{-1})	1.0×10^6–2×10^9
S	Glucose in the medium (mM)	0–35
M	Malic acid in the medium (mM)	0–12
Q	Intracellular energy (ATP) (% initial energy)	0–5
L	Lactic acid in the medium (mM)	0–35

[a] Q/N was normalized to 1 at the time of inoculation ($t = 0$). Therefore, Q/N measures energy as a percentage of the energy quota that is typically present in an overnight culture.

rately predicts the competition between *Lactococcus lactis* and the pathogen *Listeria monocytogenes* in a vegetable broth fermentation. This model included parameters for the inhibition of cell growth and metabolism due to pH and protonated lactic acid. One important prediction obtained from their competitive growth experiments was that the primary factor limiting the growth of *L. monocytogenes* in their model system was pH and not the accumulation of protonated lactic acid. This conclusion was supported by independent measurements of the parameters for pH and protonated acid sensitivity for *L. monocytogenes*. This model did, however, fail to make the mechanistic connection between nutrient acquisition and cell growth. It did not account for glucose consumption, did not predict lag or temperature effects, and relied on forcing functions to control pH dynamics.

Our objective was to develop a predictive methodology that will aid in the understanding of bacteria interacting with changing environmental factors and, ultimately, bacterial competition. We also wanted a model that embodies a more fundamental understanding of the changes that take place during the growth of a batch culture. To meet this goal, a complex mechanistic model could be used. It is well known, however, that increasing the complexity of a model may lead to poorer validation accuracy (i.e., because of a lack of parsimony). Heeding this warning, we suggest that one way to ameliorate the deficiencies in the above modeling efforts is to make a more mechanistic accounting of the cellular "energy state" with a dynamic energy budget model (14), which links nutrient consumption, energy, and growth. Thus, the work presented here is an attempt to meld the aspects of dynamic temperature change and end product inhibition into a dynamic, energy-based model describing lag, exponential, stationary, and death phases, while quantitatively revealing the mechanisms governing these features of the growth curve.

MATERIALS AND METHODS

Bacterial strains and media. *L. lactis* LA221 (chloramphenicol resistant [6]) was grown on M17 broth (Difco Laboratories, Detroit, Mich.) containing 1.5% agar (Difco), 1% glucose (Sigma Chemical Co., St. Louis, Mo.), and 5 μg of chloramphenicol/ml. Growth experiments were conducted in cucumber juice (CJ) medium (8). Cucumbers were pureed and pressed to render raw juice, which was frozen until needed. The raw juice was thawed and then clarified by heating at 85°C for 5 min, followed by centrifugation at 13,000 × *g* for 20 min, and filter sterilized. The CJ medium was prepared by adding 600 ml of juice to 400 ml of distilled water. The diluted juice was supplemented with 2% NaCl and then filter sterilized as described by Daeschel et al. (8).

Fixed-temperature experiments. Overnight cultures were prepared by growing LA221 in CJ at 30°C. Water-jacketed jars (Wheaton, Millville, N.J.) were filled with 200 ml of fresh CJ and inoculated with 10^6 CFU ml of bacterial culture^{-1}. Each flask was sealed with a silicone stopper that contained a sterile syringe sample port, through which an 18-gauge, 10-cm needle was passed. The growth medium was kept well mixed by a magnetic stirrer. Compressed nitrogen was humidified by sparging through deionized water, filtered (0.2-μm-pore-size Millex-FG50 filter; Millipore Corp., New Bedford, Mass.), and released into the headspace of the fermentor jars at a rate of 1.3 liters h^{-1}. Temperature during the fermentation was controlled by a circulating water bath (NESlab RTE-211; NESlab, Portsmouth, N.H.). The temperature of the growth medium was monitored directly by sterile thermocouples inserted through the silicone stoppers and recorded by a microcomputer (OM-3000; Omega, Stamford, Conn.). Growth observations at 10, 20, and 30°C included quantification of the number of CFU per milliliter and glucose, malic acid, and lactic acid concentrations. Growth at a particular temperature was monitored until all phases of growth had been observed.

Biological assays. A sterile disposable syringe (1 ml; Becton Dickinson, Franklin Lakes, N.J.) was used to withdraw a 1-ml sample from the fermentation flask sample port. Cells were removed from 1-ml samples by centrifugation at 13,000 × *g* for 1.5 min. High-performance liquid chromatography (HPLC) analyses of the supernatant quantified total lactic acid, glucose, and malic acid. HPLC was carried out by the single injection procedure of McFeeters (16). The pH of the medium was determined using an electronic pH meter (IQ 200; IQ Scientific Instruments, Inc., San Diego, Calif.). Cell density (number of CFU per milliliter) was determined by the spiral plate count method using an Autoplate 4000 Automated Spiral Plater (Spiral Biotech, Bethesda, Md.) and a Protos Plus Colony Counter (Bioscience International, Rockville, Md.).

Statistics and programming. All computing was performed on a 300-MHz Ultra Sparc 10 processor (Sun Microsystems, Palo Alto, Calif.). MATLAB (version 5.3) software was used to solve the differential equations described in the

TABLE 2. Model parameters

Parameter	Description (unit)	Maximum-likelihood estimate
α	Maximal bacterial growth rate (h^{-1})	3.42
μ_1	Maximal glucose consumption rate (CFU ml^{-1}) (mM^{-1})	8.95×10^{-10}
μ_2	Maximal malate conversion rate (CFU ml^{-1}) (mM^{-1})	2.41×10^{-9}
kq_1	Value of q at which cell growth rate equals $\alpha/2$ (unitless)	8.03
kq_2	Value of q at which glucose consumption rate equals $\mu_1/2$ (unitless)	1.07
kq_3	Value of q at which glucose consumption rate equals $\mu_2/2$ (unitless)	1.35×10^{-2}
δ_1	Death rate when $q = \infty$ (h^{-1})	7.02×10^{-2}
δ_2	Death rate sensitivity to changes in q (unitless)	3.73×10^3
β	Conversion rate of glucose into energy (mM^{-1} h^{-1})	6.80×10^8
γ	Energy required for cell division (CFU ml^{-1})	2.07
κ	Energy cost per 1 mM lactic acid (mM^{-1})	0.220
KT_1	Sensitivity of metabolic processes to deviations from optimal temp (h)	65.7
KT_2	Sensitivity of lactic acid inhibition to deviations from optimal temp (h)	39.5
T_{opt}	Optimal temp (°C)	30 (assumed)
τ	Energy cost for transient temp adjustment ($°C^{-1}$)	1.60×10^{-3}

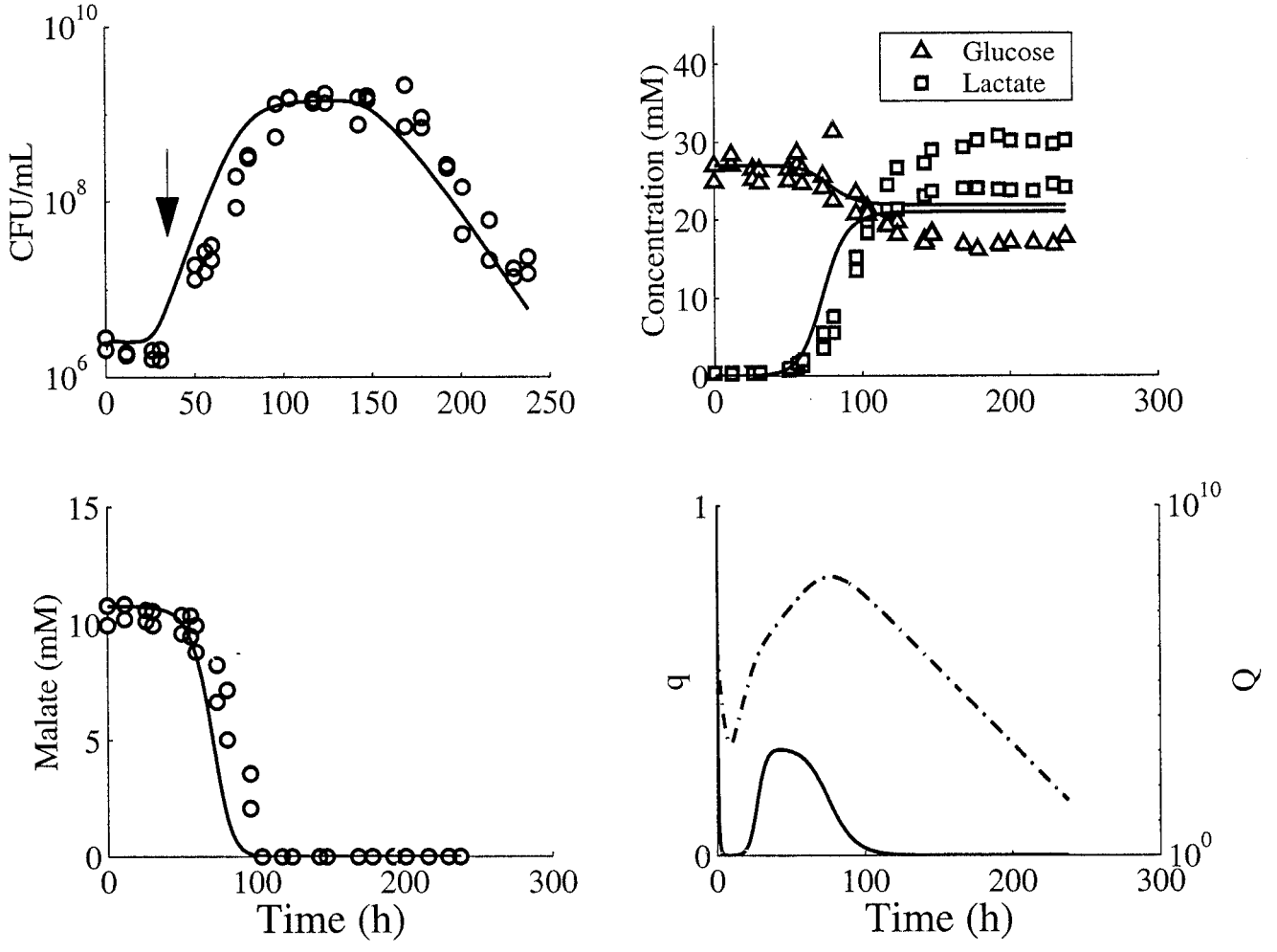

FIG. 1. Predictions of the calibrated model at 10°C. Note that the culture was incubated at 30°C prior to inoculation. The duration of lag phase is indicated by the arrow. The symbols ○ (number of CFU/milliliter or millimolar concentration of malic acid), △ (millimolar concentration of glucose), and □ (millimolar concentration of lactic acid) represent experimental values, and the curves represent predicted values. Dashed curve = Q.

Appendix and for all other programming. The equations were solved using the adaptive stiff ordinary differential equation (ODE) solver. The ODE solver often required temperatures and rates of temperature change at times different from when they were actually sampled. This problem was overcome simply by using linear interpolation to estimate the temperature values at the times requested. The derivative of temperature with respect to time was calculated when needed by using a centered finite difference approximation of the data, followed by linear interpolation to the desired time point.

Parameters were estimated using all of the fixed-temperature data at once via a maximum-likelihood method (10). We made no transformations of the data prior to parameter estimation. The data for the cell density were heteroscedastic, with sample variance approximately proportional to the magnitude of the density. A flexible distribution that has this property (constant coefficient of variation) is the gamma distribution. Schaffner (23) gives further evidence why cell count data should be considered to have a gamma distribution. The HPLC data, however, were assumed to have additive error that was normally distributed. We also assumed that the model errors were all independent, which allowed us to combine the likelihoods of all the data by simply including the log likelihoods in the same sum. We assumed that the model parameters and variance components were the same, regardless of temperature. We did, however, allow for experiment-specific variation in initial conditions. This was reasonable since the exact cell density at the time of inoculation was not known, and subsequent plate counts during the experiment provided only limited information about what this value should have been. By this method, our maximum-likelihood procedure estimates for all 14 model parameters, 4 variance components, and 20 initial conditions were calculated.

Since an adaptive ODE solver was used, neither the Jacobian nor the Hessian likelihood function depends smoothly on perturbations in the parameters (11), and traditional nonlinear least-squares algorithms failed. We used differential evolution (25), a genetic algorithm, to achieve approximate parameter estimates, followed by as many Nelder-Mead Simplex iterations as required to obtain convergence.

Validation studies. Validation of the calibrated model was accomplished by comparing predictions and data from variable environment experiments. In all cases, two or more independent replicates of the fermentations were carried out. In the first scenario, the temperature of the medium was maintained at 30°C for 3.75 h, and then it was dropped to 10°C. This temperature change was accomplished over a period of about 15 min. In order to compare the model's predictions about the impact of the previous energy state on growth, a second scenario was conducted. In this scenario, cells were grown at 30°C for 3.75 h. Then 100 μl of fermented broth was inoculated into 200 ml of fresh CJ also at 30°C. A third scenario involved a reinoculation of cells after growth into fresh medium that coincided with a temperature drop from 30 to 10°C.

Sensitivity analyses. We calculated sensitivity of a particular parameter as the relative change in the model prediction for a 10% perturbation of that parameter with all other parameters fixed at their estimated values (10). We were interested in determining the sensitivity of cell density predictions. In mathematical terms,

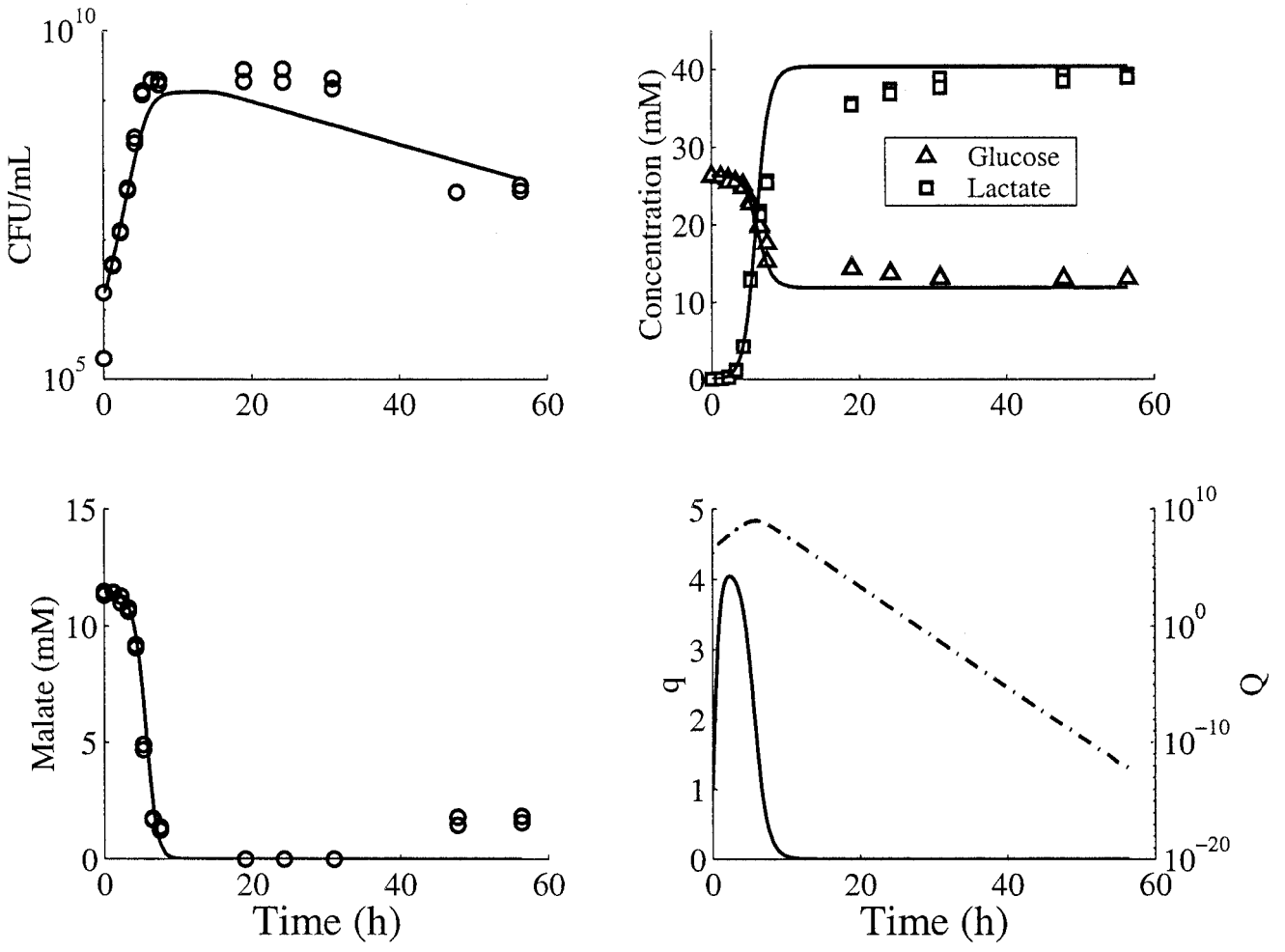

FIG. 2. Predictions of the calibrated model at 30°C. The symbols ○ (number of CFU/milliliter or millimolar concentration of malic acid), △ (millimolar concentration of glucose), and □ (millimolar concentration of lactic acid) represent experimental values, and the curves represent predicted values. Dashed curve = Q.

the sensitivity of cell density ($\log_{10} N$) to perturbations in the i^{th} parameter (P_i) was calculated as the centered finite approximation to

$$\frac{\partial(\log_{10} N)}{\partial P_i} \approx \frac{\log_{10} N|_{P_i + 0.05 P_i} - \log_{10} N|_{P_i - 0.05 P_i}}{0.1 P_i}$$

Positive values of this measure indicated that, when a parameter is perturbed upward, the model prediction for N is higher than when the unperturbed parameter is used. Conversely, negative sensitivities indicated that a positive perturbation resulted in a reduction in the predicted value for N. The advantage of this approach was that it could be performed at each point in time over a simulated fermentation. When the resulting sensitivity curve was plotted over time, it was easy to determine the relative importance of the model parameters at each of the different phases of bacterial growth.

We were also interested in the interaction between parameters that affected model predictions. To do this we used a "multiple-parameter sensitivity analysis" (26). From the analysis, we obtained the main effects, interaction terms, and higher-order terms (analogous to a multiway analysis of variance). We performed a multiple-parameter sensitivity analysis on the observed growth rate. The model described in the Appendix tracks both cell growth as well as cell death. Therefore, to determine the observed growth rate a smoothing spline was fit to the cell density data from which the first derivative was calculated. The largest positive value of the first derivative during the exponential growth phase was taken as the observed growth rate. For the analysis of variance, we used a central composite design (13), which allowed us to estimate all main effects and first-order interactions. We limited our analysis of the observed growth rate to the eight parameters determined to be important in the temporal analyses. The resulting central composite design required 273 function evaluations. P values, it should be noted, were meaningless in this context since there was technically no error in simulated data (26).

RESULTS

Model development and calibration. In the Appendix we present our model, which links the mechanisms of nutrient acquisition, end product accumulation, temperature adaptation, and cell growth. In particular, the rates of glucose consumption, malic acid reduction, and cell growth and death all depend on the present intracellular "energy" level (q). We used the convention of assigning the initial value of q to 1 because our fermentations were inoculated from overnight cultures of approximately the same age. This meant that q should be interpreted as a measure of the percentage of the initial intracellular "energy" typical in an overnight bacterial culture. The state variables of the model are summarized in Table 1, and the model parameters along with their biological interpretations and estimated values are summarized in Table 2. Malic acid was present in the medium, and malolactic con-

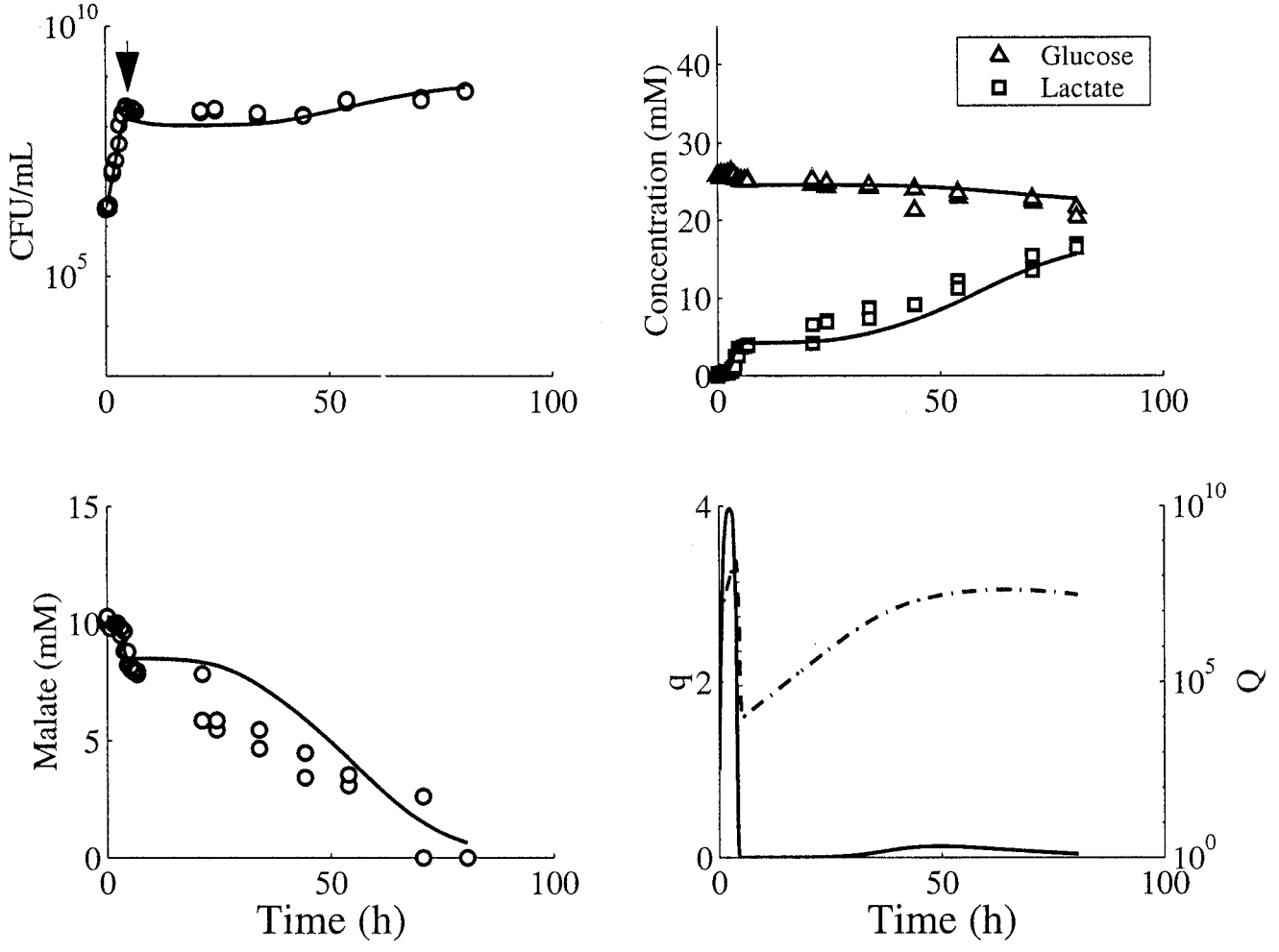

FIG. 3. Variable temperature validation (scenario no. 1). After 3.75 h, the temperature was reduced from 30 to 10°C over a period of about 15 min. Arrow indicates temperature shift. The symbols ○ (number of CFU/milliliter or millimolar concentration of malic acid), △ (millimolar concentration of glucose), and □ (millimolar concentration of lactic acid) represent experimental values, and the curves represent predicted values. Dashed curve = Q.

version of malic acid to lactic acid accounted for nearly one-third of the total lactic acid produced during the fermentation. We, therefore, included an equation for malic acid and assumed a 1:1 ratio of malic-to-lactic conversion. Energy cost due to temperature adaptation was modeled as the interaction between the deviation from the optimal temperature and the rate of temperature change. Temperature was also manifested in the model in another way. Temperatures below the optimal growth temperature (T_{opt}) should result in reductions in the growth rate, glucose consumption rate, malic acid conversion rate, and lactic acid toxicity rate. Intracellular energy should also be reduced by the costs associated with cell growth and total extracellular lactic acid concentration. Only temperatures between 10 and 30°C were considered for this model.

To calibrate the model, we chose 30°C as a reference point but also observed growth at 20 and 10°C. It is important, however, that all overnight cultures were grown at 30°C prior to inoculation for an experiment. Thus, inoculation at lower temperatures in fact constituted a temperature shock to which the bacteria had to adapt. Dependence on the rate of temperature change, as well as the magnitude of the temperature change, was manifested in the model in the equation for cellular energy, as well as in the rate-specific reductions in the glucose consumption rate, malic acid reduction rate, and lactic acid inhibition rate (see Appendix). As can be observed in Fig. 1, the shift to low temperatures produces a lag-phase effect. Cells inoculated into fresh medium at 30°C showed no lag (Fig. 2).

Model validation and analysis. After estimating the model parameters from fixed-temperature data, we validated the model against three temperature scenarios. The first scenario consisted of a variable temperature regime. Bacteria were grown for 3.75 h at 30°C, and then the temperature was brought down to 10°C over a period of approximately 15 min. Growth at 10°C was continued for another 60 h. Model predictions closely matched the experimental data. We can see in Fig. 3 that the model accurately predicted the period of rapid growth at 30°C, as well as the pronounced lag after the temperature shift.

A second scenario (Fig. 4) involved a batch growth at 30°C, followed by reinoculation into fresh medium also at 30°C. This scenario was meant to challenge the ability of the bacterial

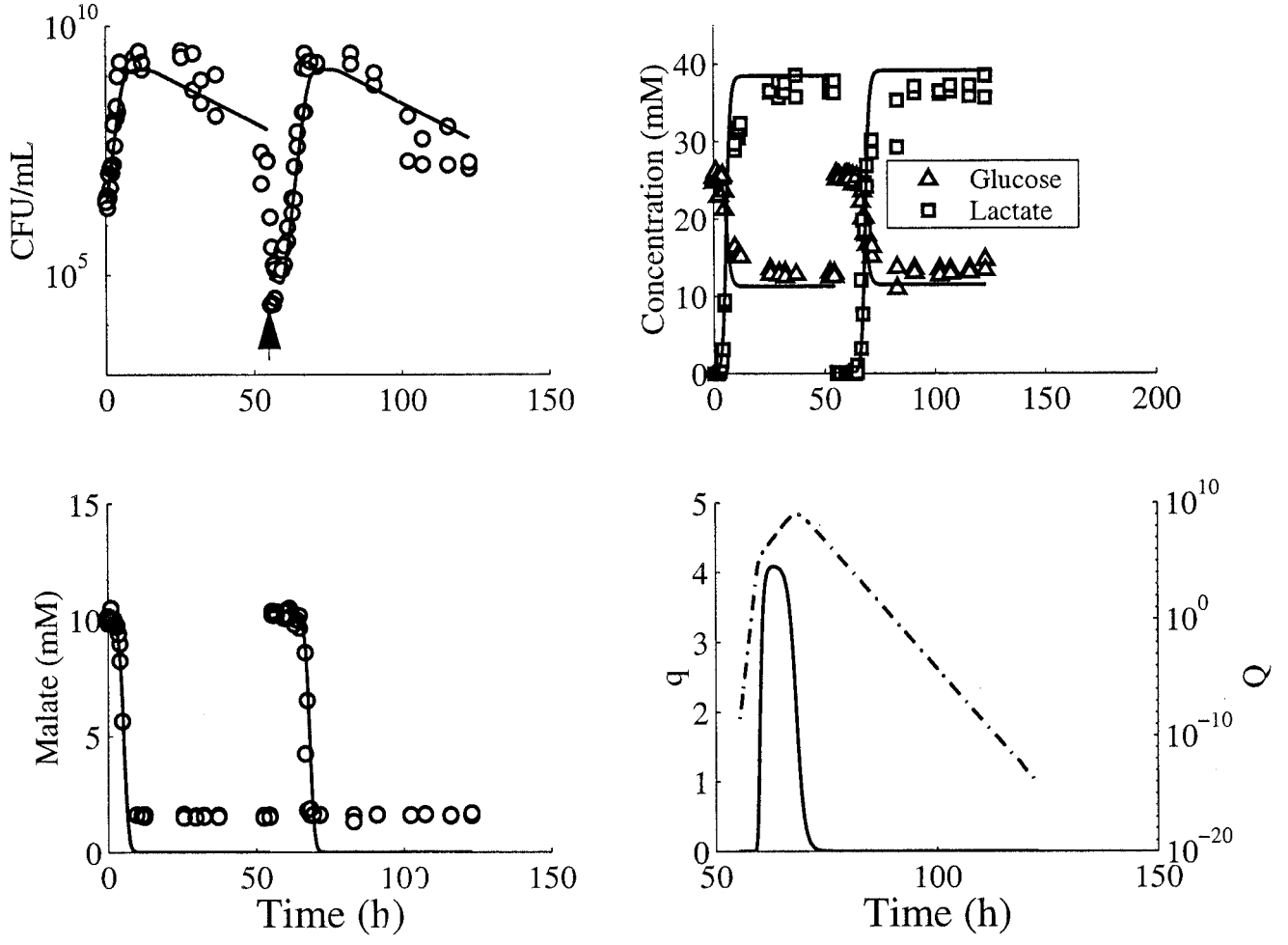

FIG. 4. Reinoculation validation experiment (scenario no. 2). After 55 h, the cells were reinoculated into fresh medium. The temperature was held at 30°C throughout the entire experiment. The symbols ○ (number of CFU/milliliter or millimolar concentration of malic acid), △ (millimolar concentration of glucose), and □ (millimolar concentration of lactic acid) represent experimental values, and the curves represent predicted values. Dashed line = Q.

population to rapidly recover from a toxic previous growth environment once placed in fresh medium. At the point of reinoculation, the model predictions for the cell counts and internal pool of energy were adjusted for dilution and used as initial conditions for a second simulation run. The energy stores of the bacteria were rapidly replenished once placed in fresh medium. There was no noticeable lag phase, and the second profile nearly duplicated the behavior of the first profile. In the third production scenario, the shift in temperature from 30 to 10°C coincided with a reinoculation into fresh medium. The results (Fig. 5) suggest an overall robustness of the model to perturbations in temperature and initial conditions.

Sensitivity analyses. We carried out a sensitivity analysis to gain insight into which components of the model are most important with respect to growth regulation in response to changes in temperature. For example, in Fig. 6 and 7, we used a "temporal sensitivity analysis" to measure sensitivity with respect to predicted cell density for the fixed-temperature fermentations. In general, the magnitudes of the sensitivities increase as the temperature decreases. At 10°C, cell counts during the exponential and stationary phases are positively affected by positive perturbations in μ_1, β_1, KT_1, and kq_1 but are negatively affected by positive perturbations in α, τ, γ, and kq_2. δ_1 is important only in death phase, where it had an increasingly negative effect. There was a reversal in the signs of all parameter sensitivities near the transition from stationary to death phase (Fig. 6). This reversal occurs to a lesser extent at 20°C (data not shown) and is absent in the analysis at 30°C (Fig. 7). Particularly striking are the curves for parameters α and kq_1, which represent growth rate and energy (respectively), and change in sign from the analysis at 10°C to the analysis at 30°C. Positive perturbations in κ (energy cost of acid stress) have a relatively larger negative effect at 30°C (Fig. 7) than at the lower temperatures (Fig. 6), and the positive perturbations of kq_1 were larger than the other parameters during the exponential and stationary phases at 30°C (Fig. 7).

While this kind of analysis is useful in exploring the effect of a single parameter, we are also interested in understanding the interplay between parameters. We found that the exponential

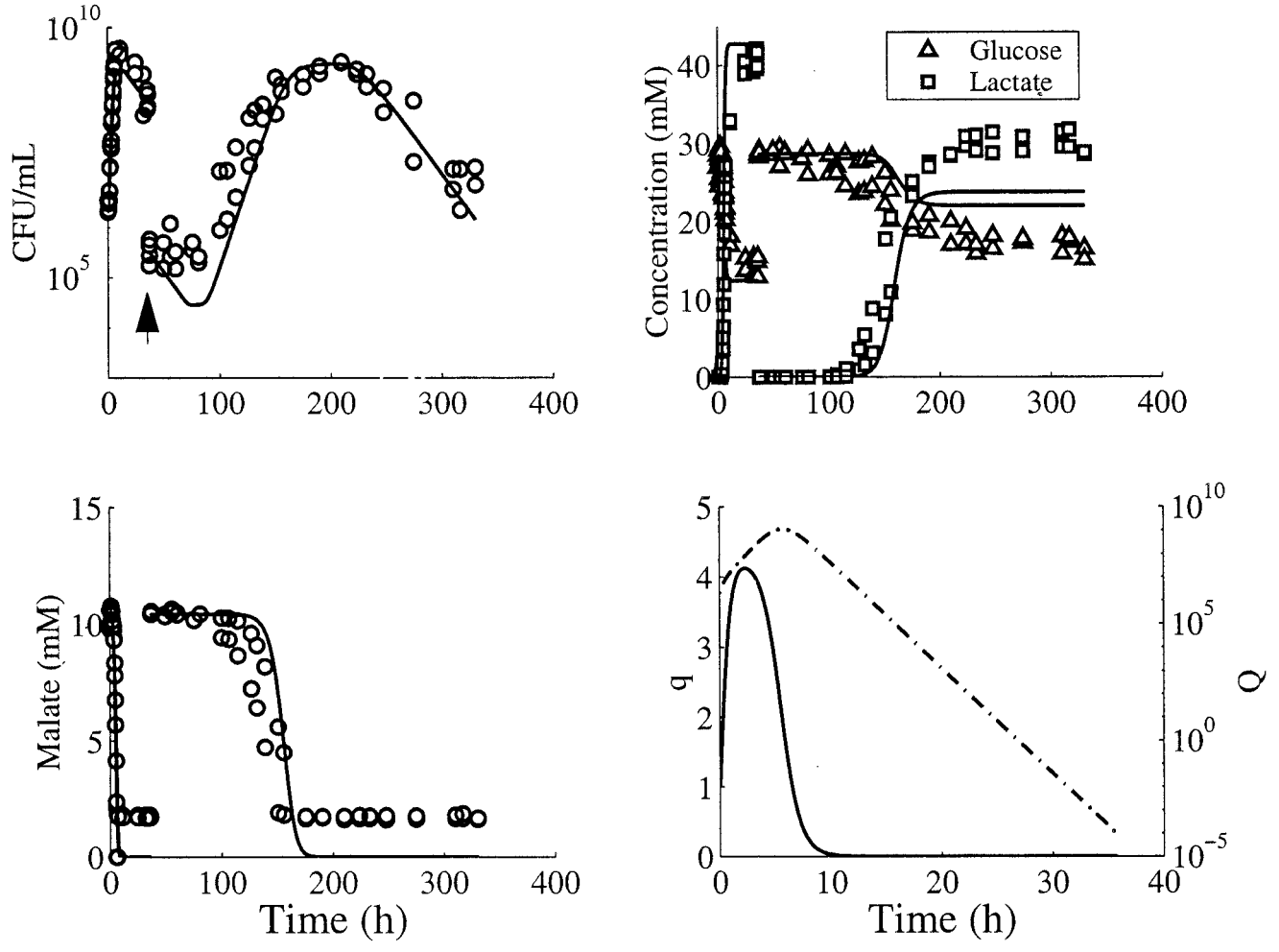

FIG. 5. Model predictions for scenario no. 3. Reinoculation into fresh medium at 35 to 75 h coincided with a shift in temperature from 30 to 10°C. The symbols ○ (number of CFU/milliliter or millimolar concentration of malic acid), △ (millimolar concentration of glucose), and □ (millimolar concentration of lactic acid) represent experimental values, and the curves represent predicted values. Dashed line = Q.

and stationary phases were most sensitive to perturbations in the parameters. Therefore, we conducted a multiple-sensitivity analysis of the maximal observed growth rate to gain a better understanding of how the model behaves during these phases of growth. The main effects, interaction terms, and second-order effects for simulations at 10 and 30°C are reported in Tables 3 and 4, respectively. Comparison of the data in Tables 3 and 4 reveals that μ_1 and β are the most important parameters in determining the growth rate. The fact that the signs of α and kq_1 in Table 4 are the opposite of what they were in Table 3 suggests that growth is limited in a manner at 10°C fundamentally different from that at 30°C. The observed growth rate, irrespective of temperature, was most strongly influenced by the glucose consumption rate (μ_1), glucose-to-energy conversion rate (β), and maximal growth rate (α). The growth rate is least affected by the energetic cost of reproduction (γ) and the energy half-saturation constant for glucose consumption (kq_2). The energetic cost of temperature adaptation (τ) is only important in the 10°C analysis (Table 4), where it tends to manifest a negative effect on growth rate through its negative interactions with μ_1, β, KT_1, and kq_1.

DISCUSSION

There is generally an inverse relationship between model complexity and model robustness (3, 10). Kooijman (14), however, argues that "a fair comparison of models should be based on the number of parameters per variable described, not on absolute number." We have developed a model that predicts not only cell density (N) but also reliably predicts glucose, lactic acid, and malic acid concentrations and gives substantive and experimentally verifiable predictions of intracellular energy using only 14 model parameters. In this regard, our model's complexity is on par with that of presently available models.

Included in Fig. 1 to 5 are the predicted internal energy profiles (Q) and the per-cell internal energy ($q = Q/N$) profiles. The model clearly predicted reductions in energy available for growth immediately after a temperature shift or when end product inhibition ensues in the stationary phase. Currently, no experiments have been conducted with *L. lactis* LA221 to support this, and this is the subject of future work in our laboratory. However, Mercade et al. (17) have shown that the yield of

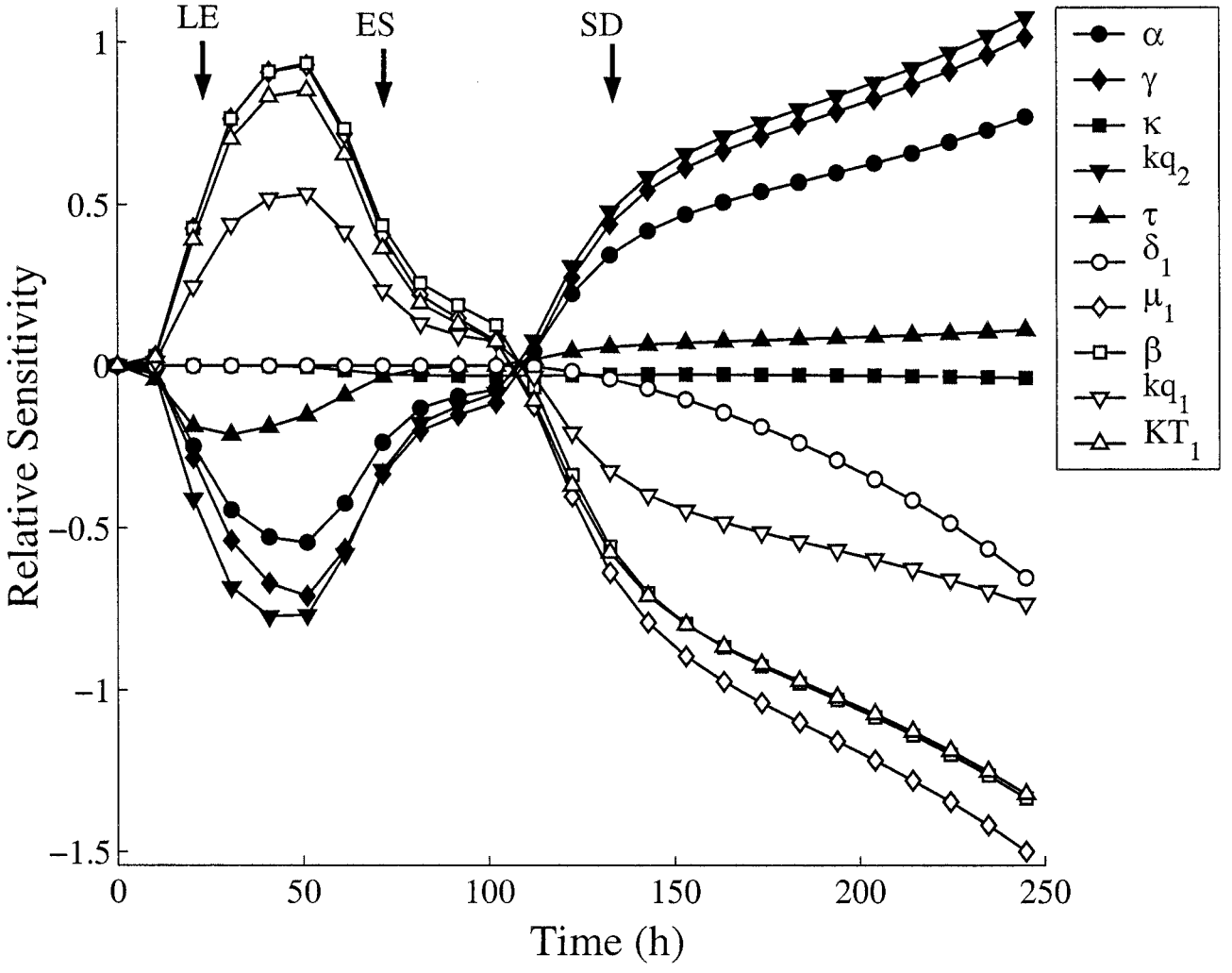

FIG. 6. Temporal sensitivity profiles of cell density ($\log_{10}$ [number of CFU/milliliter]) with respect to the model parameters at 10°C (only the 10 most sensitive model parameters shown). LE, ES, and SD are reference points indicating approximate times of transition between lag and exponential, exponential and stationary, and stationary and death phases, respectively.

ATP of *L. lactis* decreased from 11.5 g mol^{-1} at a pH of 6.6 to 5 g mol^{-1} at a pH of 4.4, thus demonstrating an energy drain due to acidic conditions. Jetton et al. (12) have shown that starved cells of *Methanothrix soehngenii* contained relatively high levels of AMP (2.2 nmol/mg of protein) but essentially no ADP or ATP during acetate degradation. Addition of new substrate, however, quickly brought the ATP levels back up to concentrations of about 1.4 nmol/mg of protein. The gram-negative bacterium *Pectinatus frisingensis* has been shown by Chibib and Tholozan (7) to experience decreases in ATP, ADP, and AMP concentrations during cold shocks (30 to 20°C). The bacteria returned to a preshock metabolic state when returned to 30°C in the presence of glucose. Metge et al. (18) showed that the total adenine nucleotide content for a species of *Pseudomonas* decreased from 153×10^{-20} mol $cell^{-1}$ during exponential phase to 56×10^{-20} mol $cell^{-1}$ during stationary phase.

Interpretation of the temporal sensitivity analyses in Fig. 6 and 7 is straightforward. By conducting the temporal sensitivity analyses at different temperatures, we were able to see how temperature affects the relative importance of each parameter in relation to model predictions. The sensitivity of α (the maximum growth rate of the cells) became negative at low temperatures, κ (the parameter that controls the energy cost of cell division) became relatively unimportant at low temperatures, and τ (energy cost for transient temperature adjustment) became important only at low temperatures. These results suggest that growth at colder temperatures was limited primarily by the requirements for temperature adaptation, while growth at 30°C was limited primarily by acid stress. These results also suggest that at low temperatures it was more advantageous to divert energy to temperature adaptation. This idea is also supported by the large negative sensitivity of parameter γ (energy required for cell division) (at 10°C) seen in Fig. 6, since it is this parameter that controls how much energy is spent on reproduction.

The sign reversal of nearly every parameter sensitivity at the end of the stationary phase in Fig. 6 is striking but entirely reasonable. This characteristic of the sensitivity analysis comes from the fact that the factors that promote strong and rapid

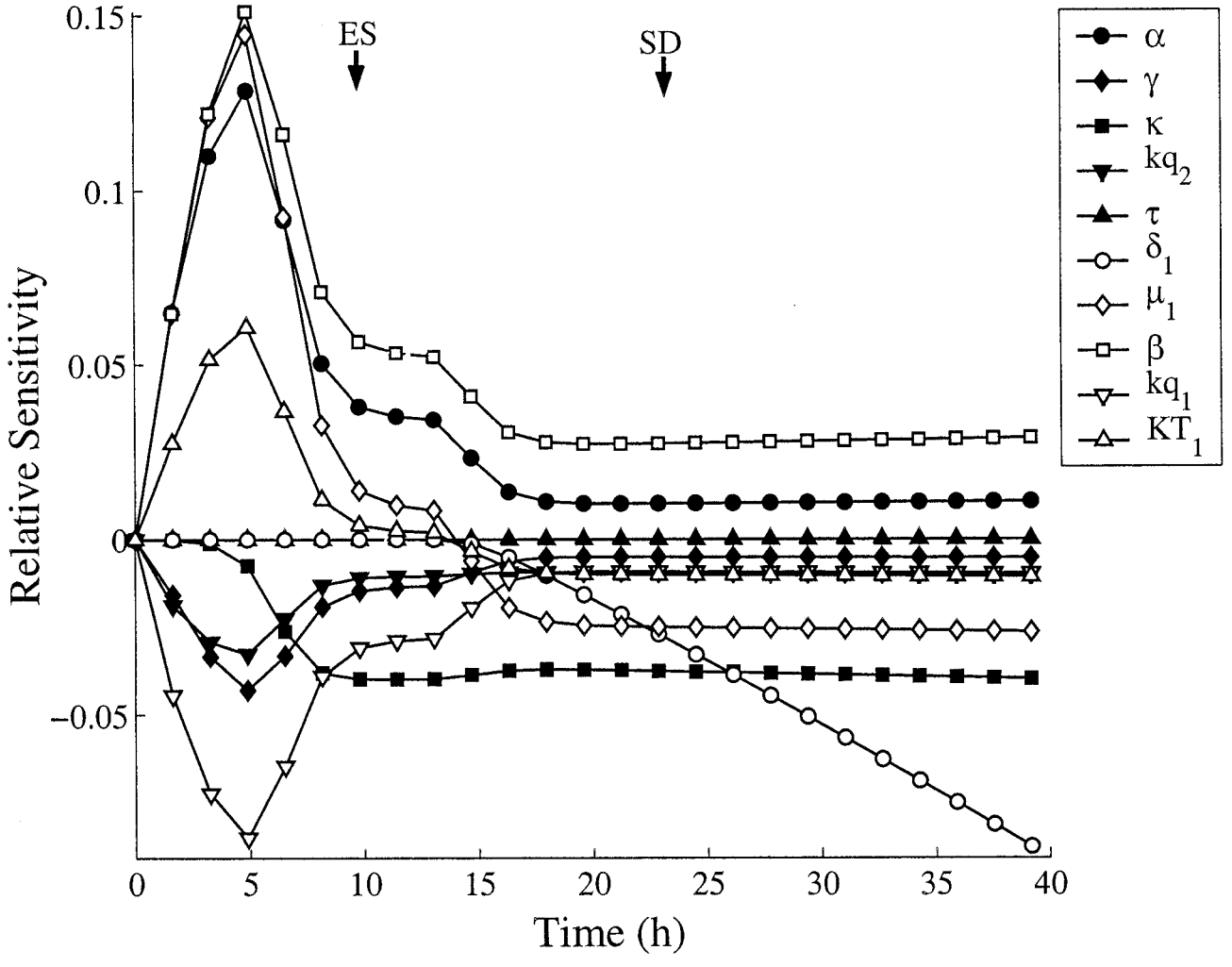

FIG. 7. Temporal sensitivity profiles of cell density ($\log_{10}$ [number of CFU/milliliter]) with respect to each of the model parameters at 30°C (only the 10 most sensitive model parameters are shown). ES refers to exponential and stationary phases; SD refers to stationary and death phases.

growth also promote rapid end product accumulation and precipitate cell death. At low temperatures, this phenomenon was enhanced by the increased energy demand required for temperature adaptation. In general, 8 of the 14 model parameters were important in determining growth during exponential and stationary phases. These were β, μ_1, KT_1, and kq_1, which have positive sensitivities, and α, τ, γ, and kq_2, which have negative sensitivities. Not surprisingly, these are the parameters that control growth (α, kq_1, and γ), sugar utilization (β, μ_1, and kq_2), and temperature adaptivity (KT_1 and τ) in the model.

TABLE 3. Multiple-sensitivity (index) analysis results for growth rate at 30°C[a]

Parameter	Constant term (main effect)	Interaction term							
		μ_1	β	KT_1	kq_1	α	τ	γ	kq_2
μ_1	**0.330**	**−0.149**	0.0626	0.0299	**−0.120**	**0.279**	0	0.0379	0.0257
β	**0.331**		**−0.145**	0.0310	**−0.119**	**0.279**	0	0.0377	0.0259
KT_1	**0.141**			**−0.102**	−0.0594	**0.126**	0	0.0165	0.0106
kq_1	**−0.167**				0.0758	−0.0386	0	0.079	0.0506
α	**0.272**					**−0.157**	0	**−0.146**	−0.0938
τ	0		Symmetric				0.010	0	0
γ	−0.0931							0.0089	−0.0189
kq_2	−0.0738								−0.0073

[a] Listed are the coefficients describing the sensitivity surface about the estimated parameters. Constant terms indicate the mean trend or "main effect" due to that parameter alone, whereas the interaction terms are a measure of how a perturbation in one of the parameters impacts model sensitivity to the other parameter involved in the interaction. The terms on the main diagonal indicate the concavity of the sensitivity surface with respect to a particular parameter. The larger values are boldfaced.

TABLE 4. Multiple-sensitivity (index) analysis for growth rate at 10°C[a]

Parameter	Constant term (main effect)	Interaction term							
		μ_1	β	KT_1	kq_1	α	τ	γ	kq_2
μ_1	**0.175**	−0.0435	**0.113**	**0.104**	−0.0863	0.0804	−0.0120	−0.0254	−0.0037
β	**0.176**		−0.0447	**0.105**	−0.0861	0.0802	−0.0123	−0.0256	−0.0038
KT_1	**0.161**			−0.0549	−0.0792	0.0738	−0.0106	−0.0227	−0.0044
kq_1	0.0972				**−0.136**	**0.196**	−0.0071	**0.140**	**0.141**
α	**−0.102**					−0.0383	0.0070	**−0.138**	**−0.141**
τ	0.0005		Symmetric				0.0266	0.0065	0.0127
γ	**−0.145**							0.0434	−0.0490
kq_2	**−0.127**								0.0073

[a] See Table 3 footnote for explanation of boldfaced values.

The multiple-sensitivity analysis of these parameters revealed that μ_1 and β were the most important parameters in determining the observed growth rate. The qualitative shift in parameter sensitivity suggests that the observed growth rate was limited in a manner at 10°C fundamentally different from that at 30°C. In particular, these results support the previous suggestion that growth was limited at low temperatures by the demand for temperature adaptation and that, at warmer temperatures, end product accumulation was the primary limiting force. For example, the parameter controlling energy cost for temperature adaptation, τ, had virtually no bearing on the model predictions at 30°C.

Previous researchers (4, 5, 9, 29, 30) have developed models to predict growth during continuous changes in temperature. These models use an empirical function, such as Gompertz or Ratkowsky relationships, to describe temperature-induced lag phase. In our model, temperature is an independent variable that controls the predicted metabolic activity of the cell. Using this mechanistic approach, we are able to predict how changes in cell physiology produce a temperature-induced lag phase. While some systematic lack of fit was observed, Fig. 1 to 5 demonstrate the qualitative agreement of predicted and experimental results. Understanding how physiological changes affect growth with varying temperatures may lead to a rational method for selecting biocontrol or starter cultures.

In this paper, we have shown that the energy costs of temperature adaptation can explain lag phase. Our model predicted lag phase, death phase, and maximal growth rates. A quadratic temperature inhibition function was used in our model; however, we may improve the functional form to allow for temperature effects above and below the optimal temperature for growth (T_{opt}). Model components did not vary independently of one another, and all affected and depended on the internal pool of cellular energy (q). It was this dynamic energy budget aspect of our model that allowed growth predictions across a range of continuously varying environmental conditions for the lag, log, and stationary phases of batch culture. Our model was validated using broth fermentations. This work may serve as the basis for modeling more complex fermentation systems. Future research will be aimed at experimentally determining intracellular ATP concentrations during batch growth of LA221.

ACKNOWLEDGMENTS

This investigation was supported in part by a research grant from USDA-NRI (Washington, D.C.), grant DMS-9805611 from the National Science Foundation (to S.R.L.), and a research grant from Pickle Packers International, Inc. (St. Charles, Ill.).

We acknowledge the technical assistance of Roger L. Thompson in the analysis of the HPLC data and Dora D. Toler for excellent secretarial assistance.

APPENDIX

Our model consists of a system of five differential equations with dependent variables for cell density (N), the extracellular concentrations of glucose (S), lactic acid (L), malic acid (M), and intracellular energy (Q). Independent variables are time t and temperature T. The model parameters and their biological interpretations, units, and estimates are given in Table 2. The differential equations are as follows:

$$\text{CFU:} \quad \frac{dN}{dt} = \alpha\left(\frac{q}{kq_1 + q}\right)N - \delta_1 \exp(-\delta_2 q)N \tag{A1}$$

$$\text{Glucose:} \quad \frac{dS}{dt} = \frac{-\mu_1}{F_{T1}}\left(\frac{q}{kq_2 + q}\right)NS \tag{A2}$$

$$\text{Malic acid:} \quad \frac{dM}{dt} = \frac{-\mu_2}{F_{T1}}\left(\frac{q}{kq_3 + q}\right)NM \tag{A3}$$

$$\text{Energy:} \quad \frac{dQ}{dt} = \beta\left[\frac{\mu_1}{F_{T1}}\left(\frac{q}{kq_2 + q}\right)NS\right] - \frac{\kappa}{F_{T2}}LQ - \gamma\left[\alpha\left(\frac{q}{kq_1 + q}\right)N\right] - \tau\left|\frac{dT}{dt}\right|(T - T_{opt})^2 Q \tag{A4}$$

$$\text{Lactic acid:} \quad \frac{dL}{dt} = 2\left[\frac{\mu_1}{F_{T1}}\left(\frac{q}{kq_2 + q}\right)NS\right] + \left[\frac{\mu_2}{F_{T1}}\left(\frac{q}{kq_3 + q}\right)NM\right] \tag{A5}$$

where

$$q = Q/N$$

$$F_{T^*} = 1 + \frac{(T - T_{opt})^2}{KT^*}$$

REFERENCES

1. **Baranyi, J., T. Roberts, and P. McClure.** 1993. A non-autonomous differential equation to model bacterial growth. Food Microbiol. **10:**43–59.
2. **Baranyi, J., and T. A. Roberts.** 1994. A dynamic approach to predicting bacterial growth in food. Int. J. Food Microbiol. **23:**277–294.
3. **Baranyi, J., and T. A. Roberts.** 1995. Mathematics of predictive food microbiology. Int. J. Food Microbiol. **26:**199–218.
4. **Bockelhurst, T., G. Mitchell, Y. Ridge, R. Seale, and A. Smith.** 1995. The effect of transient temperatures on the growth of *Salmonella typhimurium* lt2 in gelatin gel. Int. J. Food Microbiol. **27:**45–60.
5. **Bovill, R., J. Bew, N. Cook, M. D'Agostino, N. Wilkinson, and J. Baranyi.** 2000. Predictions of growth for *Listeria monocytogenes* and *Salmonella* during fluctuating temperature. Int. J. Food Microbiol. **59:**157–165.
6. **Breidt, F., and H. P. Fleming.** 1998. Modeling of the competitive growth of *Listeria monocytogenes* and *Lactococcus lactis* in vegetable broth. Appl. Environ. Microbiol. **64:**3159–3165.
7. **Chibib, N.-E., and J.-L. Tholozan.** 1999. Effect of rapid cooling and acidic pH

on cellular homeostasis of *Pectinatus frisingensis*, a strictly anaerobic beer-spoilage bacterium. Int. J. Food Microbiol. **48:**191–202.
8. **Daeschel, M. A., R. F. McFeeters, H. P. Fleming, T. R. Klaenhammer, and R. B. Sanozky.** 1984. Mutation and selection of *Lactobacillus plantarum* strains that do not produce carbon dioxide from malate. Appl. Environ. Microbiol. **47:**419–420.
9. **Fu, B., P. Taoukis, and T. Labuza.** 1991. Predictive microbiology for monitoring spoilage of dairy products with time-dependent integrators. J. Food Sci. **56:**1209–1215.
10. **Haefner, J. W.** 1996. Modeling biological systems: principles and applications, p. 180–186. Chapman & Hall, New York, N.Y.
11. **Hairer, E., S. Norsett, and G. Wanner.** 1987. Solving ordinary differential equations, p. 183. Springer-Verlag, Berlin, Germany.
12. **Jetten, M. S., A. J. Stams, and A. J. Zehnder.** 1991. Adenine nucleotide content and energy charge of *Methanothrix soehngenii* during acetate degradation. FEMS Microbiol. Lett. **84:**313–318.
13. **Keuhl, R.** 2000. Design of experiments: statistical principles of research design and analysis, 2nd ed. Duxbury Press, Pacific Grove, Calif.
14. **Kooijman, S.** 2000. Dynamic energy and mass budgets in biological systems, 2nd ed. Cambridge University Press, Cambridge, United Kingdom.
15. **Levenspiel, O.** 1980. The monod equation: a revisit and a generalization to product inhibition situations. Biotechnol. Bioeng. **22:**1671–1687.
16. **McFeeters, R.** 1993. Single-injection HPLC analysis of acids, sugars, and alcohols in cucumber fermentations. J. Agric. Food Chem. **41:**1439–1443.
17. **Mercade, M., N. Lindley, and P. Loubiere.** 2000. Metabolism of *Lactococcus lactis* subsp. cremoris MG 1363 in acid stress conditions. Int. J. Food Microbiol. **55:**161–165.
18. **Metge, D. W., M. H. Brooks, R. L. Smith, and R. W. Harvey.** 1993. Effect of treated-sewage contamination upon bacterial energy charge, adenine nucleotides, and DNA content in a sandy aquifer on Cape Cod. Appl. Environ. Microbiol. **59:**2304–2310.
19. **Monod, J.** 1949. The growth of bacterial cultures. Annu. Rev. Microbiol. **3:**371–394.
20. **Passos, F., D. Ollis, H. Fleming, H. Hassan, and R. Felder.** 1993. Modeling the cucumber fermentation: growth of *Lactobacillus plantarum*. J. Ind. Microbiol. **12:**341–345.
21. **Pruitt, K., and D. Kamau.** 1993. Mathematical models of bacterial growth, inhibition and death under combined stress conditions. J. Ind. Microbiol. **12:**221–231.
22. **Ratkowsky, D., J. Olley, T. McMeekin, and A. Ball.** 1982. Relationship between temperature and growth rate of bacterial cultures. J. Bacteriol. **149:**1–5.
23. **Schaffner, D.** 1998. Predictive food microbiology gedanken experiment: why do microbial growth data require a transformation? Food Microbiol. **15:**185–189.
24. **Skinner, G., J. Larkin, and E. Rodehamel.** 1994. Mathematical modeling of microbial growth: a review. J. Food Saf. **14:**175–217.
25. **Storn, R., and K. Price.** 1997. Differential evolution—a simple and efficient heuristic for global optimization over continuous spaces. J. Global Optim. **11:**341–359.
26. **Swartzman, G., and S. Kaluzny.** 1987. Ecological simulation primer, p. 220–223. Macmillan Publishing, New York, N.Y.
27. **Turner, M., E. Bradley, K. Kirk, and K. Pruitt.** 1976. A theory of growth. Math. Biosci. **29:**367–373.
28. **Turner, M. E., and K. M. Pruitt.** 1978. A common basis for survival, growth, and autocatalysis. Math. Biosci. **39:**113–123.
29. **Van Impe, J. F., B. M. Nicolai, T. Martens, J. D. Baerdemaeker, and J. Vandewalle.** 1992. Dynamic mathematical model to predict microbial growth and inactivation during food processing. Appl. Environ. Microbiol. **58:**2901–2909.
30. **Van Impe, J. F., B. M. Nicolai, M. Schellekens, T. Martens, and J. D. Baerdemaeker.** 1995. Predictive microbiology in a dynamic environment: a system theory approach. Int. J. Food Microbiol. **25:**227–249.
31. **Whiting, R., and M. Cygnarowicz-Provost.** 1992. A quantitative model for bacterial growth and decline. Food Microbiol. **9:**269–277.
32. **Zwietering, M., J. de Koos, B. Hasenack, J. de Wit, and K. van't Reit.** 1991. Modeling of bacterial growth as a function of temperature. Appl. Environ. Microbiol. **57:**1094–1101.